# Electronic Sensors to Detect SARS-CoV-2 Viruses in Real Time

Massood Tabib-Azar, Senior Member, IEEE, Elizabeth Middleton

Abstract— Sensors with 60 nm gap junctions coated with aptamers that bind with S1 and S2 spiking proteins of the SARS-CoV-2 virus were developed. Sensor impedance changes with virus enabling rapid (~1 min), point-of-care

detection. Exosomes and other nanoparticles in the saliva produce false positive signals but do not bind with aptamers and are easily removed to achieve 6% false positivity rates. A positive sensor voltage is used to attract the negatively charged SARS-CoV-2 virus to the junction and reduce sensor false negativity rates to below 7%. The limit of detection of the sensor is ~1000 viruses and can be altered by changing sensor's lateral dimension and its transduction noise level.





Index Terms— Biosensors, COVID-19, electrical properties, rapid detection, viruses, point-of-care

## I. Introduction

Rapid SARS-CoV-2 tests are invaluable in enabling detection and preventing the spread of COVID-19 infection [1-7]. Lateral flow antibody tests are readily available and provide results in 10-15 minutes [8-10]. Here we discuss an electronic COVID-19 sensor that provides electronic output signals for convenient readout [8-10]. The electronic sensor described here is the continuation of our work on Zika sensors [11-15] and relies on the COVID-19 spherical shape, diameter ~60-125 nm, its surface spiking proteins S1 and S2, and its negative residual charge to detect it [16,17].

Dry COVID-19 virus, like many other viruses composed of surface proteins and RNA (or DNA) inner regions, is mostly dielectric material with relative permittivity of 8-10 and very high resistivity [18,19]. Exhaled viruses and viruses in the saliva are hydrated with a thin layer of surface water. Assuming the surface water is ~10 nm thick and using the volumetric contribution of different media (water with relative permittivity of 80 at 25% of the total volume and virus with relative permittivity of 10 at 75% of the total volume) one calculates a relative permittivity of  $\varepsilon_{w+v} \sim 27$  for the hydrated virus.

Saliva is a complex biofluid consisting of 99% water and a variety of ions, including sodium, potassium, phosphates, and bicarbonate [20]. It also contains proteins, enzymes, mucins, urea, ammonia, and immunoglobulins [20]. Its pH ranges between 6.2 and 7.6 (usually it is slightly acidic) and its electrical properties *in-vivo* vary during the day [21]. Different analytes in the saliva including immunoglobulins, enzymes, and oxidation processes readily deteriorate the virus structure. The saliva samples we used in our experiments were fresh (refrigerated and not more than 3 days old). According to our

measurements, saliva conductivity increases just before meals by a factor of 2-3 in the same individual [21]. The conductivity/permittivity changes we observed between infected and uninfected saliva are usually  $\sim 5x$ .

## II. SENSOR STRUCTURE

Sensor structure in Fig. 1 was developed with the idea of trapping viruses between two electrodes and detecting them through their electrical properties [14]. It has a vertical gap that was realized using a thin oxide layer making it more suitable for nanofabrication. Our extensive atomic force microscopy (AFM) studies revealed that SARS-CoV-2 viruses in infected saliva have ~60-90 nm diameters. Thus, the gap between the two electrodes was selected to be around 60 nm to match the virus diameter.

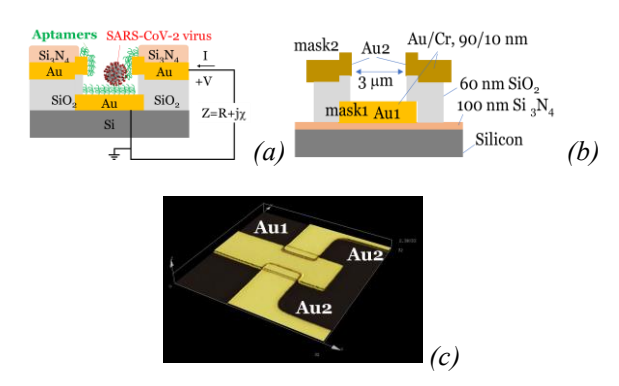


Fig. 1: a) Schematic of the sensor geometry and structure. b) Different layers and their dimensions in the sensor. c) Optical image of the sensor.

The sensor was fabricated at the nanofabrication facility of the University of Utah [22] and was functionalized with

This work was supported in part by the USTAR Program in the University of Utah.

Massood Tabib-Azar is with the Electrical and Computer Eng. Department, University of Utah, Salt Lake City, UT 84112 USA (e-mail: azar.m@utah.edu). Elizabeth Middleton is with the Department of

Internal Medicine, University of Utah, Salt Lake City, UT 84112 (e-mail: elizabeth.middleton@hsc.utah.edu)

aptamers that bind with the surface spiking proteins of SARS-CoV-2 (Fig. 1a). The aptamers are commercially available (32 base pairs from Base Pair LLC) [23] and as per manufacturer's specification have affinity of  $3.52 + /-0.17 \, nM$  with  $R^2$  value of 0.9985 as determined using biolayer interferometry technique with human saliva as buffer [23].

Fresh SARS-CoV-2 infected saliva were collected from patients in University Hospitals under study protocols approved by the Institutional Review Board of the University of Utah (IRB#: 00093575) and were transported to the sensor biosafety 2 laboratory in the engineering building. Uninfected salivae were collected from healthy tested students and other individuals.

### III. RESULTS AND DISCUSSIONS

Fig. 2 shows the change in the sensor capacitance as a function of time at 10 kHz after depositing SARS-CoV-2 infected and uninfected saliva. The sensor capacitance is larger with the infected saliva, and it becomes smaller as the viral particles bind with the sensor surface aptamers forming a dielectric layer on electrodes replacing the water molecules (saliva is 99% water) after 3-4 minutes. The output of the sensor with uninfected saliva did not show the same time dependence and was constant up to 3.5 minutes shown in here. The change in capacitance as a function of time in the infected case can be fitted with an equation  $C=C_0-at^2$  where  $C_0$  is  $1\times 10^{-9}$  F and "a" is  $7\times 10^{-11}$  F/s² with R² value of 0.9646. The saliva water evaporates in 10-15 minutes and deposits mucus and other solids on electrodes.

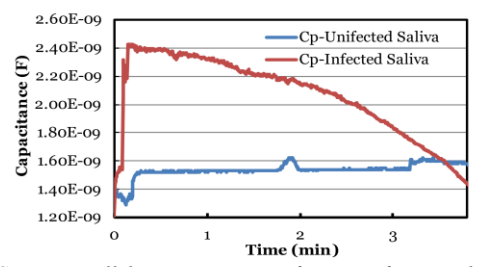


Fig. 2: Sensor parallel capacitance as a function of time with SARS-CoV-2 infected and uninfected saliva at 10 kHz.

We applied 1 ul of fresh saliva on the sensor and waited for 1 minute and then removed the excess saliva without drying the sensor. The sensor parallel capacitance (C<sub>p</sub>) in infected saliva is larger than in uninfected saliva as can be seen in Fig. 3a. The sensor resistance also changes by the hydrated viruses. Dry virus has a very large resistance and is insulating. The conductance of the hydrated virus (G<sub>v</sub>) can be estimated by considering the dc conductivity of the saliva (~1.8x10<sup>-2</sup> Siemens/cm), the gap distance between the electrodes (d~60 nm), and the effective conduction through the virus resulting in G<sub>v</sub> of 3.6x10<sup>-8</sup> Siemens. For 3000 viruses, the calculated sensor conductance becomes ~1x10<sup>-4</sup> Siemens very close to experimental values at 10 kHz. At frequencies below 100 Hz, ionic conductivities dominate and shield the virus contribution. We thus selected 10 kHz as the measurement frequency in our SARS-CoV-2 sensors.

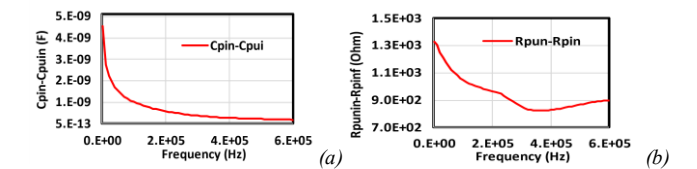
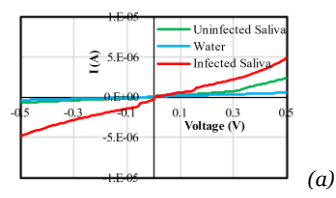


Fig. 3: a) The difference in sensor capacitance  $(C_{p\text{-infected}} - C_{p\text{-infected}})$  and b) the difference in sensor resistance  $(R_{p\text{-infected}} - R_{p\text{-infected}})$  as a function of frequency.

Even if viruses are present in the saliva, it may take them a long time to encounter the gap region of the sensor. Most viruses have residual charges depending on the pH value of their environment [24-26]. To measure the residual charge of the SARS-CoV-2 in saliva, current versus voltage (I-V) measurements were performed across the sensor (Fig. 4) with infected and uninfected saliva and de-ionized water. We have consistently observed that the infected saliva conductivity is higher (5x) than the uninfected saliva in more than 100 individuals. We have also observed that the infected saliva I-Vs are shifted near the origin as shown in Fig. 4b. In these measurements we functionalized only one of the electrodes with the aptamer leading to different I-V slopes in the 1st and the 3rd quadrants.

The average resistance in the first quadrant (away from the origin) was  $R_{e+}\sim 1.3~M\Omega$  that reduced to  $R_{e-}\sim 0.48~M\Omega$  in the third quadrant (Fig. 4b). The observed change in the cell resistance and the behavior of the I-V near the origin can be explained by assuming that the viruses are negatively charged. The aptamer coated positive electrode attracts the negatively charged viruses that form a layer of insulator increasing its effective dc resistance. Subsequently, when the other electrode that is bare is positively charged, it attracts viruses giving rise to the current in the 3<sup>rd</sup> quadrant near the origin. Within -0.01 volts corresponding to the potential needed to de-bind viruses from the aptamer-coated electrode, the magnitude of the current increases abruptly. Uninfected saliva and water do not show any of these features. The conduction path from the electrodes through the virus involved tunneling, surface channels and ionic conduction mechanisms [14].



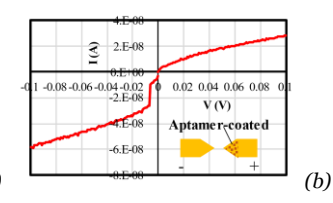


Fig. 4: Current versus voltage (I-V) measurements of a sensor with gold electrodes. Only one electrode was functionalized with aptamers. a) The infected saliva conductance is usually higher than the uninfected saliva and water. b)Near the origin the infected saliva I-V can be explained by assuming that the SARS-COV-2 virus has negative residual charge in saliva.

Fig. 5 AFM scans of the positive and negative electrode surfaces both coated with aptamers. In most cases, positive electrode surfaces contain higher density of nanoparticles than the negative electrodes. Not all these nanoparticles are SARS-CoV-2 virus, however. Many nanoparticles such as exosomes [27] and food stuff in the saliva are also negatively charged. The SARS-CoV-2 viruses in this case were around 60-90 nm in diameter.

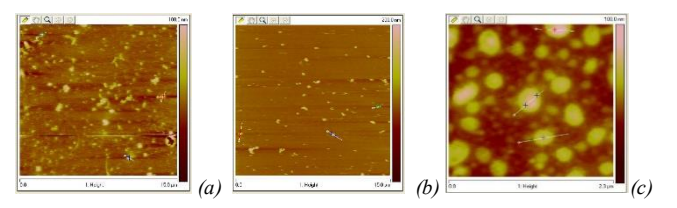


Fig. 5: 15  $\mu$ m x 15  $\mu$ m AFM scans of a) positive electrode and b) negative electrode. 60-90 nm SARS-COV-2 particles are seen in large numbers on the positive electrode. c) 2.3  $\mu$ m x 2.3  $\mu$ m AFM scan of a region in (a). In addition to the SARS-CoV-2 viruses (the larger nanoparticles) many other smaller nanoparticles are also present.

Fig. 5c shows a zoomed AFM scan of a region in Fig.5a. In addition to the SARS-CoV-2 (here around 60 nm in diameter) many other nanoparticles are present. Unlike SARS-CoV-2 viruses, all other nanoparticles lack S1 and S2 spiking proteins to bind with the sensor aptamers and they are easily removed from the sensitive gap region of the sensor.

Saliva in infected patients may additionally contain bacterial and other viral particles with 300-800 nm diameters according to our AFM studies. These do not bind with the sensor aptamers and are too large to be trapped in the sensor structure. The contribution of a single virus to the sensor output is estimated as  $\Delta C = \varepsilon_{w+v} A_{virus}/d \sim 2.4 \times 10^{-17} F$ . In a typical experiment with 1 μL of infected saliva, we observed a change of around 0.1x10 <sup>9</sup> F that when divided by the above  $\Delta C$  gives an estimated number of viruses of around  $4.2x10^6$ . Assuming a moderate detection capability of 0.1 pF in the sensor capacitance, the limit-of-detection for the above sensor can be estimated to be around 1000 viruses. Many techniques can detect 10<sup>-18</sup>–10<sup>-15</sup> F but require long integration time to reduce the contribution of the environmental noise. The noise in our sensor was around 0.05 pF. Figure 6 shows C<sub>p</sub> in 54 sensors with infected and uninfected fresh saliva samples.

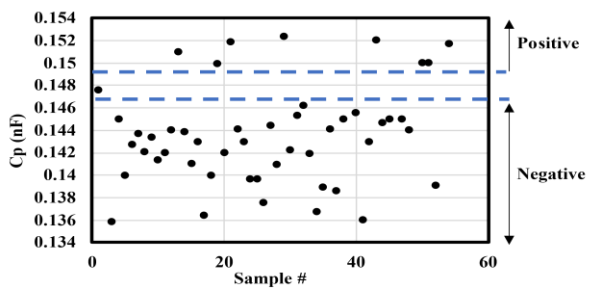


Fig. 6: Sensor capacitances at 10 kHz in sensors with different saliva samples. In these experiments, we used 54 fresh saliva samples of which 7 were infected.

The false positivity rate of our sensor is around 6% and its false negativity rate is around 7% in the laboratory environment. Its main source of false detection are other bio nanoparticles such as exosomes and comparable food particles in the saliva. Soot particles and other airborne carbon containing nanoparticles can also contribute. However, these nanoparticles do not bind with the sensor aptamers, and their electrical properties are different than the SARS-CoV-2 virus. The virus density in the immediate vicinity of the sensor junction gap is directly proportional to the viral load in the saliva that varies in individuals and in the course of the infection.

Acknowledgement: This work was partially supported by an NSF RAPID grant and financial support from the University of Utah Research Corporation. The sensors described in this work are being commercialized by the University of Utah. Dr. Aaron Duffy can be contacted (email address: <a href="mailto:aaron.duffy@utah.edu">aaron.duffy@utah.edu</a>) for further information.

#### REFERENCES

- Chaibun, T., Puenpa, J., Ngamdee, T., Boonapatcharoen, N., Athamanolap, P., O'Mullane, A. P., Lertanantawong, B. (2021). Rapid electrochemical detection of coronavirus SARS-CoV-2. *Nature Communications*, 12(1), 802 (810 pp.). doi:10.1038/s41467-021-21121-7
- Lik-Voon, K., Chia-Yu, C., Sheng-Yu, H., Pei-Wen, W., Choon-Han, H., Chung-Te, L., Chia-Ching, C. (2021). Development of flexible electrochemical impedance spectroscopy-based biosensing platform for rapid screening of SARS-CoV-2 inhibitors. *Biosensors and Bioelectronics*, 183, 113213 (113210 pp.). doi:10.1016/j.bios.2021.113213
- Mahshid, S. S., Flynn, S. E., & Mahshid, S. (2021). The potential application of electrochemical biosensors in the COVID-19 pandemic: A perspective on the rapid diagnostics of SARS-CoV-2. *Biosensors and Bioelectronics*, 176, 112905 (112910 pp.). doi:10.1016/j.bios.2020.112905
- Minghan, X., Carey, P. H., Fares, C., Fan, R., Siang-Sin, S., Yu-Te, L., Pearton, S. J. (2020). Rapid Electrochemical Detection for SARS-CoV-2 and Cardiac Troponin I Using Low-Cost, Disposable and Modular Biosensor System. Paper presented at the 2020 IEEE Research and Applications of Photonics in Defense Conference (RAPID), 10-12 Aug. 2020, Piscataway, NJ, USA.
- Pan, D., Alafeef, M., Dighe, K., & Moitra, P. (2020). Rapid, Ultrasensitive, and Quantitative Detection of SARS-CoV-2 Using Antisense Oligonucleotides Directed Electrochemical Biosensor Chip. ACS Nano, 14(12), 17028-17045. doi:10.1021/acsnano.0c06392
- Rashed, M. Z., Kopechek, J. A., Priddy, M. C., Hamorsky, K. T., Palmer, K. E., Mittal, N., Williams, S. J. (2021). Rapid detection of SARS-CoV-2 antibodies using electrochemical impedance-based detector. *Biosensors and Bioelectronics*, 171, 140-145. doi:10.1016/j.bios.2020.112709
- Vadlamani, B. S., Uppal, T., Verma, S. C., & Misra, M. (2020). Functionalized TiO2 nanotube-based electrochemical biosensor for rapid detection of SARS-CoV-2. Sensors, 20(20), 5871 (5810 pp.). doi:10.3390/s20205871
- Daming, W., Shaogui, H., Xiaohui, W., Youqin, Y., Jianzhong, L., Shimin, W., Yuguo, T. (2020). Rapid lateral flow immunoassay for the fluorescence detection of SARS-CoV-2 RNA. *Nature Biomedical Engineering*, 4(12), 1150-1158. doi:10.1038/s41551-020-00655-z
- Wang, D., He, S., Wang, X. et al. Rapid lateral flow immunoassay for the fluorescence detection of SARS-CoV-2 RNA. Nat Biomed Eng 4, 1150–1158 (2020). https://doi.org/10.1038/s41551-020-00655-z
- 10.T. Nicol, C. Lefeuvrea, O. Serria, A. Piverta, b, F. Joubaudc, V. Dubéed, A. Kouatchetf, A. Ducancell, F. Lunel-Fabiania, H. Le Guillou-Guillemettea, "Assessment of SARS-CoV-2 serological tests for the diagnosis of COVID-19 through the evaluation of three immunoassays: Two automated immunoassays (Euroimmun and Abbott) and one rapid lateral flow immunoassay (NG Biotech)." Journal of Clinical Virology Volume 129, August 2020, 104511. doi.org/10.1016/j.jcv.2020.104511.
- 11.Dolai, S., Baker, B., & Tabib-Azar, M. (2021). Micro Fabricated MEMS Colorimetric Devices to Measure Zika-Induced Residual Stress and Mass Loading. *IEEE Sensors Journal*, 21(4), 4682-4687. doi:10.1109/JSEN.2020.3029536
- 12.Dolai, S., Hsuan-Yu, L., Magda, J., & Tabib-Azar, M. (2018). Metal-Oxide-Hydrogel Field-Effect Sensor. Paper presented at the 2018 IEEE Sensors, 28-31 Oct. 2018, Piscataway, NJ, USA.
- 13.Dolai, S., & Tabib-Azar, M. (2020). 433 MHz lithium niobate microbalance aptamer coated whole Zika virus sensor with 370 Hz/ng sensitivity. *IEEE Sensors Journal*, 20(8), 4269-4274. doi:10.1109/JSEN.2019.2961611
- 14.Dolai, S., & Tabib-Azar, M. (2020). "Microfabricated Nano-Gap Tunneling Current Zika Virus Sensors with Single Virus Detection Capabilities." *IEEE Sensors Journal*, 20(15), 8597-8603. doi:10.1109/JSEN.2020.2984172
- Dolai, S., & Tabib-Azar, M. (2021). "Zika Virus Field Effect Transistor." IEEE Sensors Journal, 21(4), 4122-4128. doi:10.1109/JSEN.2020.3029535.
- 16.M. Tabib-Azar, S. McKellar, C. Furse, "Free Space Resonant Electromagnetic Sensing Techniques to Detect Airborne Viral and Environmental Particles Using Atomic Layer Graphene." NT21: International Conference on the Science and Application of Nanotubes and Low-Dimensional Materials. Proc., p. 65 (2021).
- 17.M. Tabib-Azar, "Electronic Spiking Protein-Based COVID Sensors." 2021 Meet. Abstr. MA2021-01 2036. https://iopscience.iop.org/article/10.1149/MA202101522036mtgabs/meta
- 18.A. Cuervoa, P. D. Dans, J. L. Carrascosa, M. Orozco, G. Gomila, and L. Fumagalli, "Direct measurement of the dielectric polarization properties of

DNA," PNAS E3624–E3630, www.pnas.org/cgi/doi/10.1073/pnas.1405702111\

- 19.R. I. MacCuspie, N. Nuraje, Sang-Yup Lee, A. Runge, and Hiroshi Matsui, "Comparison of Electrical Properties of Viruses Studied by AC Capacitance Scanning Probe Microscopy." J Am Chem Soc. 2008 January 23; 130(3): 887–891. doi:10.1021/ja075244z.
- 20.S. P. Humphrey, and Russell T. Williamson, A review of saliva: Nomal composition, flow, and function THE JOURNAL OF PROSTHETIC DENTISTRY, VOLUME 85 NUMBER 2, p 162-169.
- 21. Nahid Antu and M. Tabib-Azar, unpublished work.
- 22.U of Utah Nanofabrication facility: https://www.nanofab.utah.edu/
- 23.Base Pair LLC. https://www.basepairbio.com/
- 24.K. S. Zerda, C. P. Gerba, K. C. Hou, and S. M. Goyal, "Adsorption of Viruses to Charge-Modified Silica, Vol. 49 (1), p 91-95 (1985).
- 25.X. Mi, E. K. Bromley, P. U. Joshi, F. Long, and C. L. Heldt, "Virus Isoelectric Point Determination Using Single-Particle Chemical Force Microscopy, Langmuir 2020, 36, 370–378.
- 26.S. Karlin and V. Brendel, "Charge configurations in viral proteins," Proc. Natl. Acad. Sci., Vol. 85, pp. 9396-9400 (1988).
- 27.S. Sharma, H. I. Rasool, Viswanathan Palanisamy, Cliff Mathisen, Michael Schmidt, D. T. Wong, and J. K. Gimzewski, "Structural-mechanical characterization of nanoparticles- Exosomes in human saliva, using correlative AFM, FESEM and force spectroscopy." ACS Nano. 2010 April 27; 4(4): 1921–1926. doi:10.1021/nn901824n.



Massood Tabib-Azar received M.S. and Ph.D. degrees in electrical engineering from the Rensselaer Polytechnic Institute in 1984 and 1986, respectively. In 1987 he joined the faculty of EECS department at Case Western Reserve University. He was a fellow at NASA during 1992-1992, on Sabbatical at Harvard University during 93-94, at Yale University

during 2000-2001, at UC Berkeley during 2015-16, and at the Massachusetts Institute of Technology in 2016. He was a Program Director at the ECCS Division of National Science Foundation during 2012-2013 Academic Year. Massood is currently a USTAR Professor of ECE at the University of Utah, Electrical and Computer Eng. Department with an adjunct appointment in Bioengineering Department. His current research interests include nanometrology, micro-plasma devices, nano-electromechanical computers, novel devices based on solid electrolytes (memristors), sensors and actuators, injectable bio-systems, quantum sensing, and quantum computing. His teaching interests include development of courses in electronic device physics and electromagnetics with an emphasis on solving problems and the use of computer-aided instruction tools. He is author of three books, two book chapters, more than 270 journal publications, and numerous conferences proceeding articles. He has introduced and chairs many international symposia in his fields of interest. He is in the Editorial Board of IEEE Electron Device Letter Dr. Tabib-Azar is a recipient of the 1991 Lilly Foundation Fellowship and he is a member of the New York Academy of Sciences, IEEE (Electron Devices), APS, AAPT, and Sigma Xi research societies. He has also received more than 14 certificate of appreciation and recognition for his professional activities and a best paper award from Design Automation conference in 2001 for his work on electromagnetic properties of interconnects and defects in ICs, a best paper award from International Conference on Intelligent Robots and Systems in 2004 for his work on Human-Machine Interface, and a best paper award from ISQED for his work on NEMS Processors in 2011.